Canadian Mineralogist
Vol. 26, pp. 193-208 (1988)

INVESTIGATIONS OF THE STILLWATER COMPLEX.
IV. THE ROLE OF VOLATILES IN THE PETROGENESIS OF THE J-M REEF, MINNEAPOLIS ADIT SECTION

ALAN E. BOUDREAU
Department of Geological Sciences, AJ-20, University of Washington, Seattle, Washington 98195, U.S.A.

ABSTRACT

Extensive activity of Cl-rich aqueous fluids in the genesis of the olivine-rich rocks of olivine-bearing zone I (OBZ I) of the Stillwater Complex, in Montana, host of the PGE-bearing J-M Reef, is evident in the relative abundance of Cl-rich hydrous phases and the common occurrence of pegmatitic textures. Polymineralic inclusions of hydrous and anhydrous minerals in chromite and apatite are interpreted to have crystallized from trapped volatile-rich melt. The presence of anorthositic zones around layered and podiform segregations of olivine-rich rocks are interpreted as metasomatic zones because they are commonly monomineralic, have sharp contacts with neighboring rocks, and have separate mineral assemblages that are not in equilibrium. A Cl-rich, PGE-bearing volatile fluid migrating through a largely solidified cumulate sequence can be redissolved in stratigraphically higher, hotter intercumulus melt that is vapor-undersaturated. This would localize volatile enrichment to a particular zone and result in partial melting of the cumulates. Modal and textural data are consistent with a model in which progressive interaction of a (gabbro)norite + interstitial melt protolith with volatile fluid led to the following sequence of reactions: olivine was produced by incongruent melting of pyroxene, and incomplete melting of plagioclase produced round, reverse-zoned grains. Chromium, liberated during the destruction of pyroxene, was precipitated as chrome spinel. With increasing fluid/rock ratio, phlogopite and other hydrous phases were eventually precipitated, whereas chrome spinel became unstable and was reprecipitated outward of the fluid-rich areas. This reaction sequence was accompanied by a decrease in the fugacities of both oxygen and sulfur.

Keywords: platinum-group elements, Stillwater Complex, Montana, J-M reef, chlorine, hydrated phases, spinel.

SOMMAIRE

Une activité importante d'une phase fluide riche en chlore semble indiquée dans la genèse de roches riches en olivine de la zone OBZ I du massif de Stillwater (Montana), qui renferme le banc J-M à concentrations en éléments du groupe du platine. Cette activité explique l'abondance relative de phases hydratées riches en Cl et le développement d'une texture pegmatitique. Des inclusions polymétalliques de minéraux anhydres et hydratés dans la chromite et l'apatite seraient dues au piégeage de goutelettes de magma enrichi en composants volatils. Les zones anorthositiques autour de ségrégations litées et en lentilles de roches riches en olivine seraient des zones métasomatiques parce qu'elles sont généralement monominéraliques, et qu'elles montrent un contact franc avec les roches avoisinantes et qu'elles séparent les assemblages de minéraux avec lesquels elles se sont pas équilibrées. Une phase fluide riche en Cl et porteuse des éléments du groupe du platine pourrait, après migration au travers des cumulats déjà formés, être repris en solution à un niveau plus élevé dans la séquence par un liquide intercumulus qui se trouve à température plus élevée et sous-saturé en eau. Ce mécanisme limiterait l'enrichissement en composants volatils à une zone particulière, et pourrait mener à une refonte des cumulats. Les données modales et texturales concordent avec un modèle dans lequel il y a interaction progressive d'un assemblage de (gabbro)norite et de bain fondu interstitiel avec une phase fluide, qui a donné la séquence de réactions suivante: formation de l'olivine par fusion incongruente du pyroxène, fusion partielle du plagioclase, ce qui explique les cristaux arrondis et à zonation inverse. Le chrome, libéré lors de la destruction du pyroxène, apparaît sous forme de spinelle chromifère. Avec une augmentation du rapport de fluide à roche, phlogopite et autres phases hydratées sont éventuellement apparues, tandis que le spinelle a été déstabilisé et remobilisé vers les zones externes riches en fluide. Une diminution dans la fugacité de l'oxygène et du soufre aurait accompagné cette séquence de réactions.

(Traduit par la Rédaction)

Mots-clés: éléments du groupe du platine, complexe de Stillwater, Montana, banc J-M, chlore, phases hydratées, spinelle.

INTRODUCTION

Several recent papers have shown that the stratabound platinum-group element (PGE)-bearing zones of the Bushveld Complex (the Merensky Reef and the UG-2 chromitite) have been affected by Cl-rich, high-temperature hydrothermal fluids (*e.g.*, Schiffries 1984, Johan & Watkinson 1985, Ballhaus & Stumpfl 1985a, b, c, 1986). In addition, Boudreau *et al.* (1986) showed that the hydrous minerals of the main PGE zone of the Stillwater Complex (the Howland Reef, or J-M Reef; Bow *et al.* 1982, Todd *et al.* 1982) are similarly Cl-rich and argued that the ore zones in both intrusions were levels at which Cl-rich aqueous fluids, exsolved during the solidification of the lower cumulate sequence, were trapped at a chemical and physical discontinuity within the cumulate pile. Boudreau *et al.* (1986) suggested that the high Cl/F ratios which characterize these zones can occur when Cl-bearing volatile fluids migrate upward through the cumulate pile to redissolve in stratigraphically higher, hotter intercumulus melts which are fluid-undersaturated.

An expected consequence of the redissolution of fluid in the interstitial melt is that the melt cannot have remained in equilibrium with the original cumulate assemblage, and that certain rocks are representative of more extensive interaction with volatile-enriched melt than are others. In this paper, field, petrographic, and geochemical evidence for

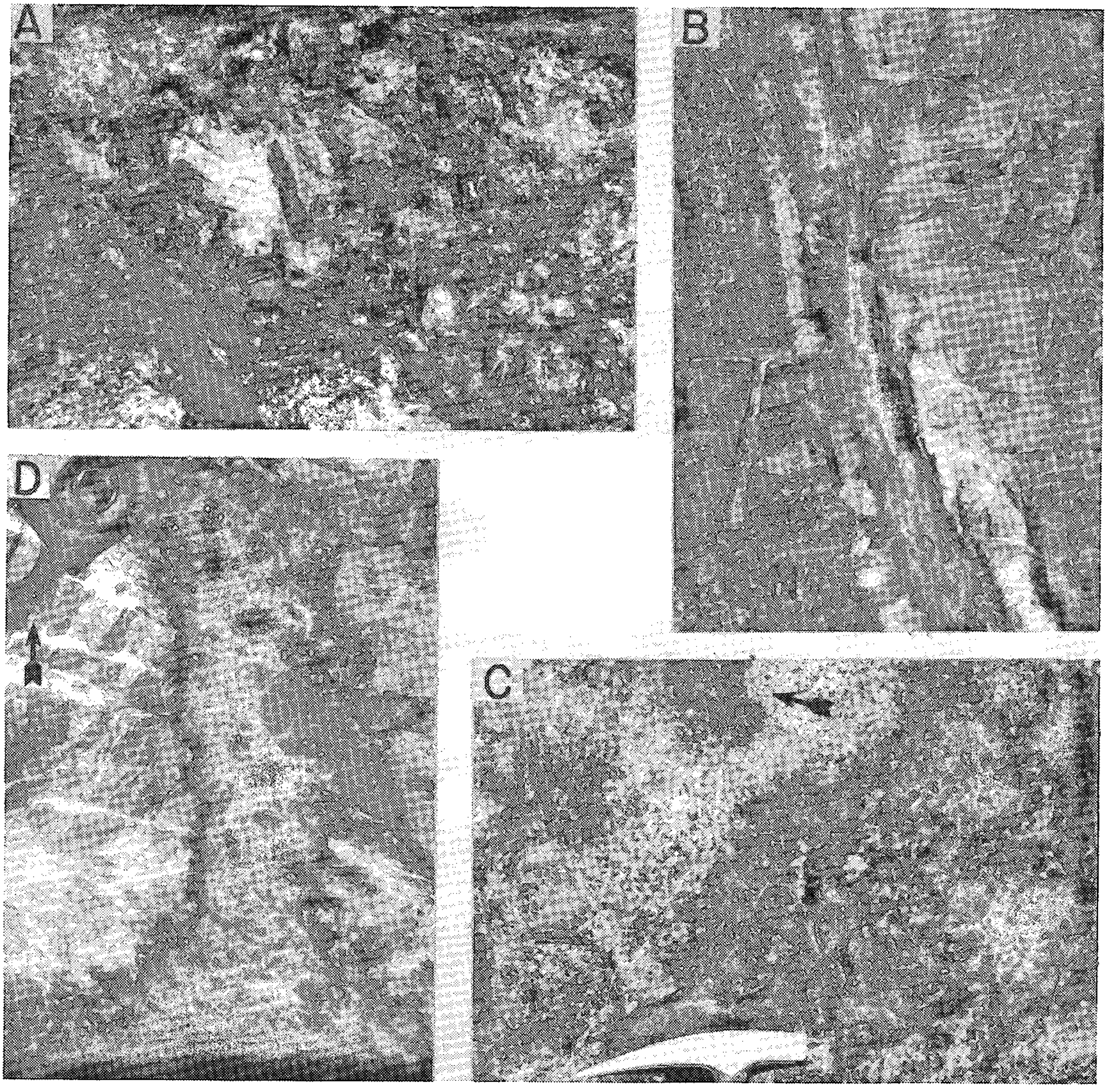

FIG. 1. Features of OBZ I and vicinity. Clockwise from top left: A) Massive sulfide, composed predominantly of pyrrhotite, pentlandite, chalcopyrite and accessory PGE-bearing phases. Sulfides (light-colored region) form the core to a plagioclase–orthopyroxene pegmatite immediately below the first occurrence of olivine in the Minneapolis adit. Preserved within the massive sulfide are casts of large silicate (pyroxene?) crystals (*e.g.*, just above and to the right of the lens cap). B) Thin olivine-bearing layer (dark) and the associated anorthositic selvages (light) developed within norite (N), Minneapolis adit. Arrow points up-section. The olivine-bearing layer is now sheared and partly serpentinized. Note that as the olivine-bearing layer thins toward the top of the photograph, so also do the accompanying anorthosites, particularly the upper (leftmost) anorthosite. C) Pegmatitic mafic segregation (lower right) and surrounding medium-grained anorthositic rock, Minneapolis adit. Arrow points up-section. D) An apophysis of an olivine-rich layer (dark), intruded into overlying anorthosite, Minneapolis adit. Arrow points up-section.

TABLE 1. MODAL DATA FOR ROCKS FROM OBZ I, MINNEAPOLIS ADIT

SAMPLE	plag	olivine	opx	cpx	sulfide	chromite	phlog
MA503	99.4	-	-	0.2	0.4	-	-
MA203	90.7	-	2.0	7.0	0.3	-	tr
MA168	90.1	-	1.1	5.3	3.5	-	-
MA187	89.2	-	10.8	-	-	-	-
MA185	88.0	0.3	0.5	11.3	tr	-	-
MA186	87.1	-	2.6	6.3	4.0	-	-
MA159A	86.0	-	13.8	0.2	-	-	-
MA168	85.0	-	4.2	8.3	2.5	-	tr
MA152	85.0	-	0.1	13.7	1.3	-	-
MA208	82.8	14.4	2.4	0.4	tr	-	-
MA119	81.5	16.1	4.0	-	0.7	-	-
MA197	80.7	-	0.1	13.1	6.1	-	tr
MA209	79.4	-	20.3	0.3	tr	-	-
MA189	71.8	1.3	25.5	1.4	-	-	-
5104ERAC	70.5	15.1	6.6	5.7	2.0	-	-
MA191	70.6	-	16.8	2.0	10.6	-	-
MA161	68.6	-	24.7	6.6	-	-	-
MA190	64.9	1.5	9.7	23.9	-	-	-
5108EN	63.9	33.3	3.1	-	0.1	-	-
MA205	62.8	25.9	3.3	7.0	-	1.0	0.1
MA204	56.7	34.1	5.3	2.4	0.2	1.3	tr
5108EK	49.2	37.0	9.4	2.1	1.1	1.3	-
MA212	41.8	48.4	3.0	0.5	5.2	1.2	tr
MA198	35.0	29.3	32.3	0.5	5.1	2.5	-
MA206	34.2	57.7	4.1	0.5	0.1	3.3	0.1
MA106A	33.5	59.4	2.9	1.4	-	2.8	-
5104WL	16.1	53.9	17.5	5.5	1.4	-	1.4
MA109A	15.9	74.1	0.4	2.5	1.8	-	5.3
MA110	15.5	70.7	5.7	0.9	0.6	-	6.7
5104WL	11.8	73.4	2.3	0.3	9.7	-	2.5
5108EN2	11.0	41.2	45.1	-	2.1	0.2	0.4
MA119'	10.1	67.6	16.3	0.4	1.6	-	4.1
5104EX	2.4	66.5	20.0	0.6	1.8	-	10.1

Modes based on 1000(+) points per thin section. Abbreviations: plag plagioclase, opx orthopyroxene, cpx clinopyroxene, phlog phlogopite (+ minor apatite and amphibole), tr trace amounts observed but not intersected in counting traverse.

subliquidus melting, recrystallization and metasomatism within the Minneapolis adit section of the J-M Reef is reviewed. The observed reef assemblages are interpreted as the result of partial melting in response to fluid exsolved from lower in the cumulate pile and trapped along a vapor-undersaturated discontinuity. A semiquantitative model is presented in which rock sequences, mineral modes, and geochemical trends are interpreted in terms of increasing reaction progress (*i.e.*, increasing fluid/rock ratio) as hot volatile-rich fluid reacts with a fluid-undersaturated melt + cumulate protolith.

GENERAL GEOLOGY OF THE J-M REEF

The general geology and stratigraphy of the Reef sequence have been described elsewhere (Conn 1979, McCallum *et al.* 1980, Bow *et al.* 1982, Todd *et al.* 1982, Barnes 1983, Barnes & Naldrett 1985, 1986, Mann & Lin 1985, LeRoy 1985, Mann *et al.* 1985, Turner *et al.* 1985). Only a brief summary of the general features is given here. Nomenclature and stratigraphic subdivisions are those of McCallum *et al.* (1980), except that the Ultramafic and Banded zones are termed series to conform with current usage.

The J-M Reef is a zone of PGE and sulfide mineralization that can be traced across the exposed strike length of the Stillwater Complex at a level approximately 400 m above the base of the Banded series. The Reef is contained within olivine-bearing zone I (OBZ I) in which lithologies range from anorthosites to a variety of olivine- and chromite-bearing rocks, with lesser amounts of norites, gabbronorites and orthopyroxenites; significant lateral variations in rock type cause small-scale complexity. The rocks between the top of the Ultramafic series and the base of OBZ I consist of a lower, relatively homogeneous plagioclase–bronzite cumulate (Norite zone I, or N I) overlain by a zone in which cumulus augite is modally abundant (Gabbronorite zone I, or GN I). The hanging wall of OBZ I consists of a lower norite unit and an upper gabbronorite unit (zones N II and GN II).

The relative increase in pegmatitic rock types and hydrous phases (*e.g.*, phlogopite) in OBZ I relative to footwall and hanging-wall lithologies is evidence

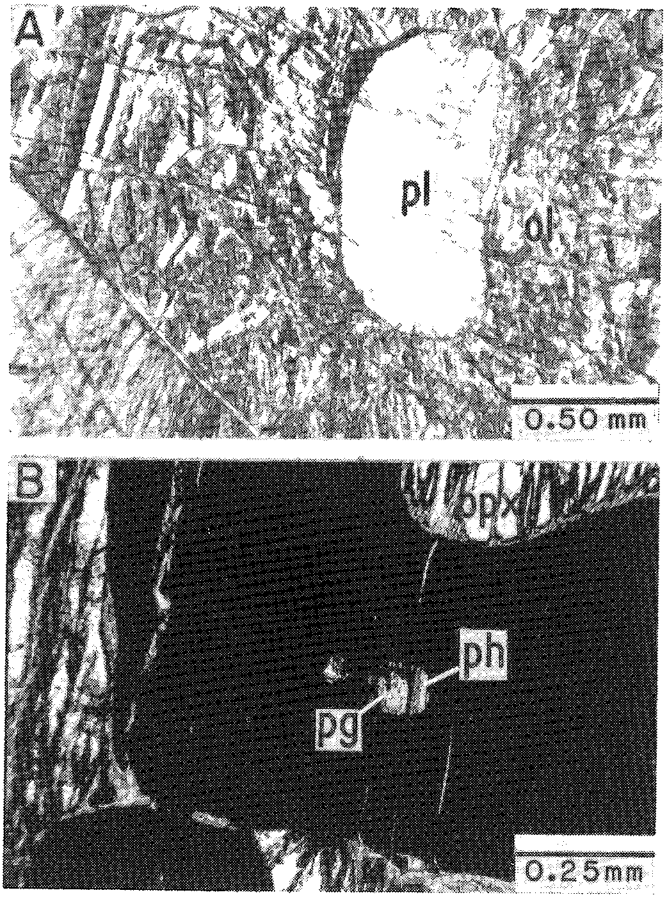

FIG. 2. A) A round, kidney-shaped plagioclase grain (pl) enclosed in olivine (ol) extensively altered to serpentine + magnetite. B) Round chromite grain with inclusions of phlogopite (ph) and pargasite (pg). The chromite itself is enclosed in partly altered orthopyroxene (opx).

for a significant role of volatiles within this zone. In some instances, the pegmatites may be quite spectacular, with massive PGE-bearing sulfide present in the cores of silicate pegmatites (Fig. 1a).

The rocks of OBZ I in the Minneapolis adit area show a marked segregation of mafic from felsic phases. In general, there is a spatial relationship between the olivine-rich rocks (troctolites and dunites) and anorthosite. This association is present both as anorthositic selvages developed about olivine-rich layers (Fig. 1b) and as podiform accumulations of olivine within an anorthositic host (Fig. 1c). In the best examples, medium-grained anorthosites are asymmetrically developed about a coarse-grained to pegmatitic olivine-rich rock with the anorthosites developed more thickly above olivine-rich layers than below. Similar anorthosites may also be developed around olivine-rich segregations within troctolites. Within norites or gabbronorites, the thickness of the anorthositic layers is proportional to the thickness of the associated olivine-bearing layer. Furthermore, the anorthositic selvages may thin and disappear as the associated olivine layer thins and disappears. Locally, the olivine-bearing rocks may form apophyses in the surrounding anorthosites (Fig. 1d). The mafic pods are typically olivine-rich, although locally coarse pyroxene, which encloses olivine and other earlier phases, may be the predominant mafic phase. In both the layered and podiform cases, the contacts between anorthosite and the olivine-rich rocks are generally sharp. The texture of olivine varies from interstitial to euhedral at the contact. The podiform, olivine-bearing rocks are stratabound on a scale of tens of meters, and, as such, can be mapped as a separate, laterally "continuous" layer of mixed lithologies (Turner *et al.* 1985). Locally, the podiform zones grade into the layered olivine/anorthosite association.

PETROLOGIC AND GEOCHEMICAL EVIDENCE FOR VOLATILES AND SUBLIQUIDUS REACTIONS IN THE OLIVINE-BEARING ROCKS OF OBZ I

McCallum *et al.* (1980) noted that hydrous phases, particularly biotite, are most frequently associated with the olivine-bearing rocks of the Banded series. The correlation between the abundance of olivine and hydrous minerals is evident in the modal data from the Minneapolis adit (Table 1), where phlogopite, amphibole (pargasite and pargasitic hornblende), and apatite are relatively abundant in olivine-rich rocks, but are rare in rocks with less than approximately 20% olivine. Furthermore, phlogopite and other hydrous phases occur only rarely as accessory minerals in (gabbro)norite or anorthosite of the Lower Banded series and in other cumulate rock of OBZ I, even where these rocks are proximal to the olivine-bearing rocks. Sulfides (pyrrhotite + pentlandite + chalcopyrite ± pyrite and a variety of PGE-bearing phases, *e.g.*, Bow *et al.* 1982) occur in all rock types, but are most common in coarse-grained olivine-rich rocks and in adjacent troctolitic and anorthositic rocks (*e.g.*, Bow *et al.* 1982, Mann & Lin 1985).

Plagioclase

Plagioclase is present both as cumulus grains and, in the coarser-grained olivine-rich rocks, as coarse-grained interstitial material. Plagioclase inclusions are present in olivine in rocks that contain cumulus plagioclase. In addition, cumulus plagioclase within the olivine-bearing rocks has an irregular, subspherical habit, indicating that plagioclase has been resorbed (Barnes & Naldrett 1986) (Fig. 2a). Furthermore, these same grains show a tendency to be reversely zoned, whereas plagioclase from the surrounding anorthosites, norites and gabbronorites are, as a rule, normally zoned (Fig. 3). These features in the cumulus plagioclase of the olivine-bearing rocks of OBZ I are consistent with preferential dissolution of the albite component from plagioclase by one of several mechanisms. Mixing of plagioclase-phyric melts with plagioclase-undersaturated melt can lead to resorption of plagioclase (Barnes & Naldrett 1986). However, the relative abundance of hydrous phases associated with the olivine-bearing rocks and the local, podiform nature of the rocks suggest alternative explanations. Addition of volatiles to a volatile-fluid-undersaturated melt + crystal assemblage can lower the plagioclase liquidus and solidus temperatures to produce partially resorbed, reversely zoned cumulus grains. Alternatively, plagioclase may dissolve incongruently in silica-poor aqueous fluids and result in reversely zoned grains (*e.g.*, Adams 1968, Orville 1972, Schiffries 1982). In the J-M Reef environment the fluids are likely to have been Cl-bearing (Boudreau *et al.* 1986), suggesting the reverse-zoning may occur via the following exchange reaction with a volatile-rich fluid (v) (Orville 1972):

$$\underset{\text{plagioclase}}{2NaAlSi_3O_8} + CaCl_{2,v} \rightarrow \underset{\text{plagioclase}}{CaAl_2Si_2O_8} + 2NaCl_v + 4SiO_{2,v} \quad (1)$$

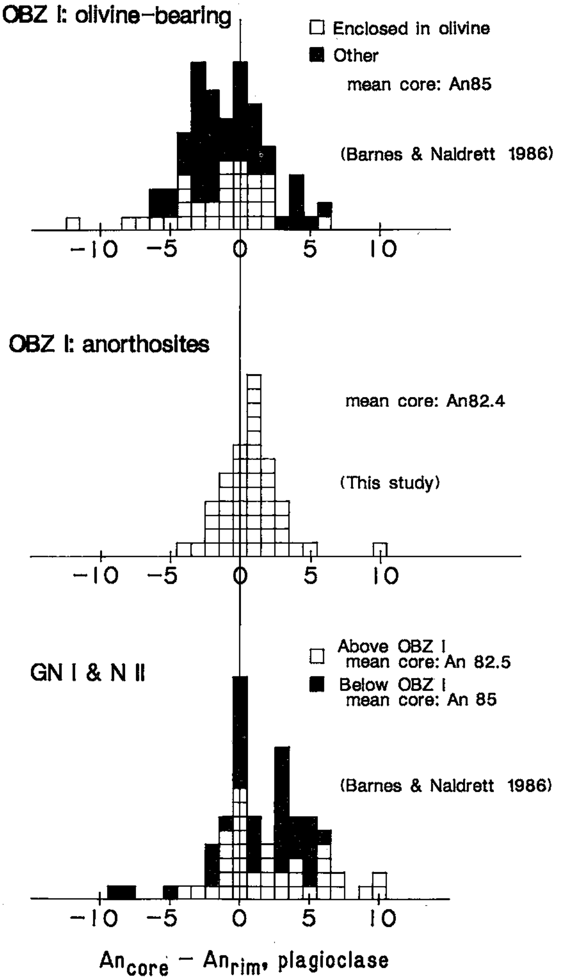

FIG. 3. Histogram of (An$_{core}$ − An$_{rim}$) compositions in cumulus plagioclase from OBZ I and vicinity, as determined by electron microprobe. Top and bottom histograms are after Barnes (1983). Samples that plot to the left of the center line are reverse-zoned, whereas those samples which plot to the right of the center line have normal zoning.

These textual and compositional observations are consistent with dissolution and loss of cumulus plagioclase by reaction in the olivine-rich rocks.

Since iron can be incorporated in plagioclase as both ferrous and ferric iron, variation in the total iron content may be a useful indication of relative variation in oxygen fugacity (Longhi *et al.* 1976). Alternatively, variations in the iron content of plagioclase may reflect temperature of crystallization, as the iron content of plagioclase decreases with decreasing temperature of crystallization (*e.g.*, Smith 1983). A plot of total iron (as FeO) in plagioclase against the Mg/(Mg + Fe) ratio of associated mafic minerals is presented in Figure 4. All cumulus plagioclase from OBZ I, as well as interstitial plagioclase in rocks that do not contain phlogopite, lie along a broad trend that shows increasing iron content in plagioclase with increasing iron content of associated mafic minerals, parallel to the trend for Stillwater cumulus plagioclase as defined by McCallum (1968). However, interstitial plagioclase from the phlogopite-bearing assemblages coexists with relatively iron-rich olivine, and is significantly lower in total iron, consistent with the phlogopite-bearing assemblages having crystallized at a lower oxygen fugacity. Alternatively, the plagioclase may have crystallized at a lower temperature, owing to depression of the liquidus and solidus in a volatile-enriched melt.

Chromite

Chromite, present as disseminated grains in rocks with greater than about 20% olivine, is generally absent in anorthosites and olivine-poor troctolites. In the West Fork Adit area ("the waterfall section"), a distinctive thin chromite-rich layer occurs at the contact between the coarse-grained to pegmatitic olivine-rich rocks and the surrounding anorthositic rocks (Todd *et al.* 1982, Mann *et al.* 1985). Similar chromite-rich margins are commonly associated with the pegmatites of the Ultramafic series (Raedeke & McCallum 1984) and with pegmatitic rocks near the Driekop dunite pipe of the eastern Bushveld Complex (Schiffries 1982).

In some cases, the chromite grains are round or have embayments, again suggesting partial resorption (Barnes 1983) (Fig. 2B). Furthermore, chromite is rare in olivine-rich rocks with abundant phlogopite (Table 1). The textural observation, the low chromium content of the phlogopite and other phases in chromite-free olivine-bearing rocks (Boudreau *et al.* 1986), and the local occurrence of chromite at the margins of the olivine-rich pegmatite are consistent with local mobilization of chromium.

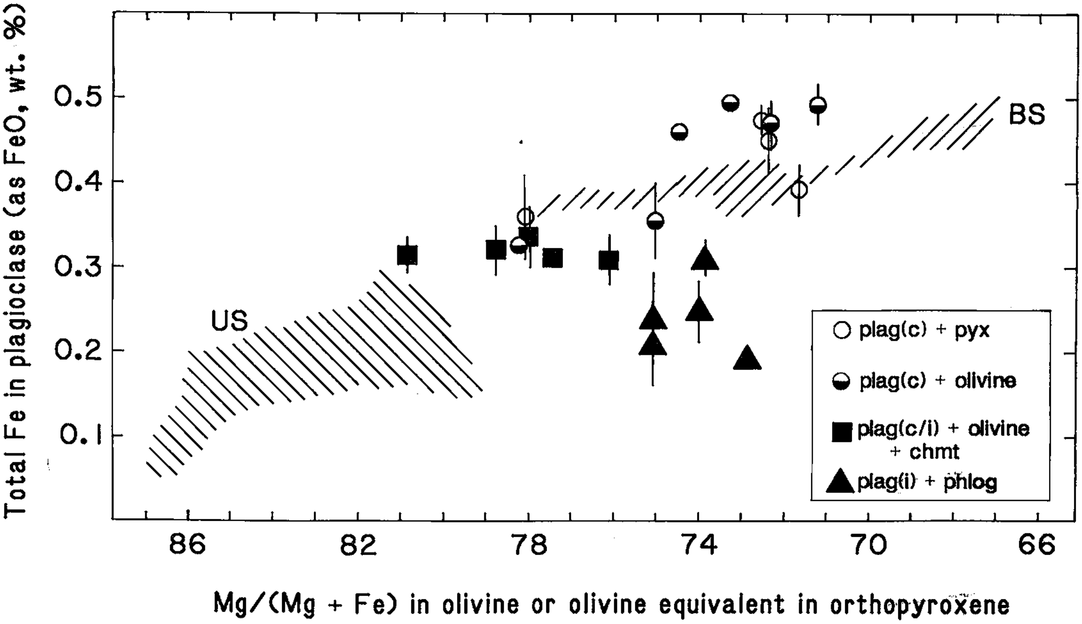

FIG. 4. Total iron in both cumulus and interstitial plagioclase (as FeO, wt. %), against the molar Mg/(Mg + Fe) ratio in olivine or the olivine-equivalent molar Mg/(Mg + Fe) ratio in orthopyroxene. Abbreviations: plag plagioclase, pyx pyroxene, chmt chrome spinel, phlog phlogopite, c cumulus, i interstitial. The Mg/(Mg + Fe) ratio of samples which contained orthopyroxene only was calculated to an equivalent Mg/(Mg + Fe) ratio in olivine using a $K_D = (X_{Fe}/X_{Mg})_{opx}/(X_{Fe}/X_{Mg})_{ol} = 0.88$ (from Barnes 1983). Diagonally ruled areas labeled "US" and "BS" are fields defined by the data of McCallum (1968) for the Ultramafic series and Banded series, respectively. Chromite occurs with both interstitial and cumulus plagioclase. Error bars show the total range observed, where they exceed the symbol size.

Commonly present within chromite grains are polymineralic inclusions of phlogopite, pargasite, and less common orthopyroxene and serpentinized olivine (Barnes 1983) (Fig. 2b). Similar inclusions occur in the apatite from OBZ I (Boudreau *et al.* 1986). The presence of negative crystal faces in the host crystal, and the observation that the host crystal may be included within yet another silicate phase, are consistent with the interpretation that these inclusions grew from what was initially a trapped inclusion of hydrous melt (Barnes 1983, Boudreau *et al.* 1986). A hopper-shape morphology present in some of the chromite grains suggests that the melt was trapped during rapid growth of the host chromite and that a hydrous melt was present at the time the chromite nucleated. Similar inclusions have been reported in the iron-rich chrome spinel of the hortonolite pipes of the Bushveld Complex (Stumpfl & Rucklidge 1982).

DISCUSSION

Irvine *et al.* (1983), Campbell *et al.* (1983), Barnes (1983) and Barnes & Naldrett (1985) have proposed that the Howland Reef and the rocks of OBZ I formed during the mixing of two compositionally distinct parent magmas, although Irvine *et al.* proposed a mixing mechanism significantly different from the other models. However, the evidence presented above for volatiles, the spatial relationship between the olivine-bearing rocks and the accompanying anorthosites, and the apparent instability of cumulus plagioclase in the olivine-bearing rocks suggest that an *in situ* development of these rocks should also be considered. It is proposed that the scale of the segregations, the coarse-pegmatitic textures of the olivine-rich rocks, and the high chlorine concentrations in phlogopite and apatite associated with the olivine-rich rocks are the result of reactions and mass transfer involving localized concentrations of a Cl-rich volatile fluid or a volatile-enriched melt phase. The anorthosites that separate olivine-bearing rocks from gabbronorites or norites show features typical of metasomatic zones in that they are commonly monomineralic, show relatively sharp contacts with the surrounding rocks and, as shown below, separate mineral assemblages that are not in equilibrium.

The effect of volatile addition to a vapor-undersaturated melt + crystal assemblage: phase diagram considerations

The lack of any reversal in the composition of cumulus plagioclase and pyroxenes to more primitive compositions at the level of OBZ I (Todd *et al.* 1982, Barnes & Naldrett 1985), the presence of abrupt lateral terminations of olivine-bearing rocks (Bow *et al.* 1982, Turner *et al.* 1985) and the evidence presented above suggest an alternative explanation for the reappearance of olivine in OB I. That is, olivine may have formed from pre-existing cumulus pyroxene as a consequence either of incongruent dissolution at subsolidus temperatures (*e.g.*, Bowen & Tuttle 1949, Cameron & Desborough 1964, Schiffries 1982), or by incongruent melting induced by volatile fluxing in which a fluid added to a vapor-undersaturated melt + crystal assemblage lowered the liquidus and solidus temperatures. The latter possibility is discussed below.

Addition of H_2O will expand the phase field of olivine with respect to pyroxene (*e.g.*, Kushiro *et al.* 1968, Kushiro 1975). In the case of an unsolidified pile of cumulates, the subliquidus relationships can be visualized by considering a volatile fluid (evolved during the solidification of stratigraphically lower cumulates) that migrates upward (by its own buoyancy) and redissolves in a hotter, melt–crystal assemblage that has not yet crystallized to a point of fluid saturation. Redissolution and entrappment of the fluid is likely to occur at a stratigraphic discontinuity within the cumulate sequence, initially produced by an influx of a volatile-poor, more primitive magma. This situation is suggested by the change from a three-phase gabbronorite of the footwall of OBZ I to the two-phase norite which comprises the hanging wall. Alternatively, the process of constitutional zone refining in layered intrusions (McBirney 1987) is an analogous mechanism by which volatile-enriched zones and melting may occur spontaneously in a thick zone of *in situ* crystallization.

The production of olivine from pyroxene during volatile fluxing is illustrated by the isothermal phase relations in the system $Fo–SiO_2–H_2O$ (Fig. 5). Consider a nearly solid protolith consisting of enstatite and a small amount of melt of composition "M", which has not yet solidified to a point where it would evolve a volatile-fluid phase. The bulk composition of the crystal–melt assemblage will lie on a tieline connecting the enstatite and melt compositions. Consider two bulk compositions, denoted P_1 and P_2, which differ only in the relative amounts of melt and enstatite present. Addition of volatile fluid to the fluid-undersaturated interstitial melt will cause the bulk compositions to change along the dotted "volatile-mixing lines" of Figure 5 and will result in the melting of enstatite. Note, however, that the presence of the liquid field prevents a separate vapor phase from being present above the level of the discontinuity in the cumulate pile until all the solid assemblage has melted, as long as the temperature remains constant (or nearly so). If fluid is added to the interstitial melt along a thin zone, then the surrounding rocks above and below the volatile-enriched zone can act as a thermal buffer by supplying the necessary heat of fusion for the above reaction by

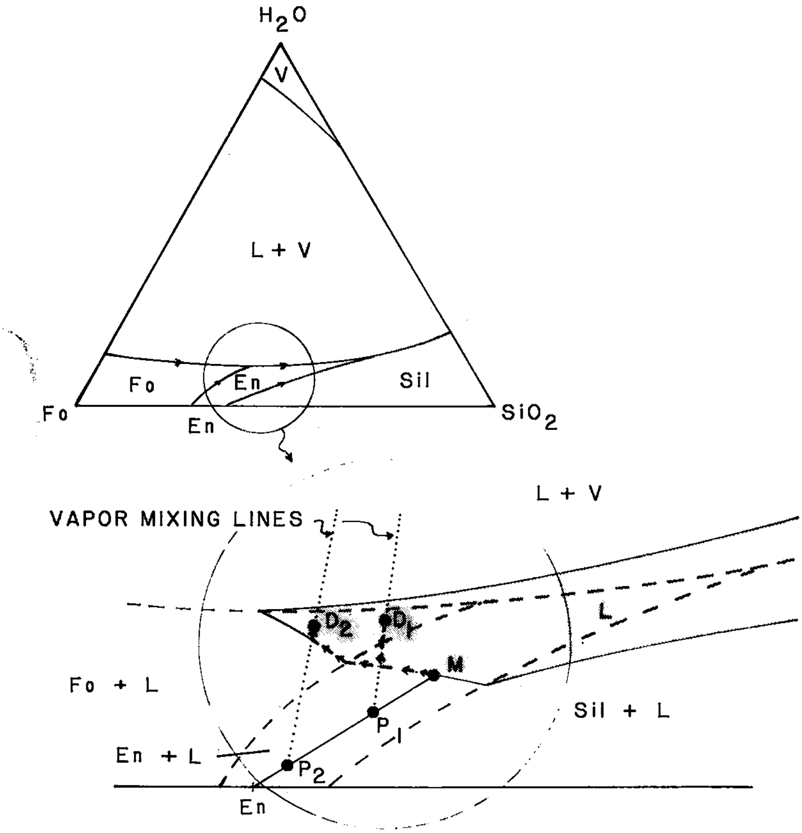

FIG. 5. The system $Fo–SiO_2–H_2O$. Abbreviations: Fo forsterite, En enstatite, Sil silica, L liquid (melt), V volatile fluid. The bottom half shows a detail of the isothermal phase relations near the $Fo–SiO_2$ join; the isothermal liquidus-field area is shown shaded. The phase relations are, in part, schematic, after the 10 kbar phase diagram of Kushiro *et al.* (1968). The extent of the volatile-fluid field at the H_2O apex expands down the $H_2O–SiO_2$ join with increasing pressure. Also, the location of the Fo–En boundary moves to the right of the enstatite composition on the $Fo–SiO_2$ join at low pressure. See text for further details.

crystallizing a thermally equivalent amount of melt. The melt composition will change along an isotherm on the liquidus surface, as shown by the heavy dashed lines. For the initial bulk composition P_1, all enstatite will melt before the melt composition reaches the boundary with olivine, and hence any further addition of fluid will change the melt composition along a volatile-mixing line. The final composition of the melt shown, D_1, lies within the forsterite field such that, on eventual cooling, olivine will be the first mineral to crystallize. The melt composition could follow the volatile-mixing line all the way to fluid saturation, but olivine would still be the first mineral to precipitate. In either case, however, all pyroxene must melt and the system must cool before any olivine is produced. For bulk composition P_2, however, melting of enstatite is halted at the olivine–enstatite boundary until all enstatite is converted into olivine. With continued influx of fluid, all olivine is melted, and the melt composition moves into the liquid field along a fluid-mixing line, giving a final composition shown (D_2). At low pressures, only a few weight percent H_2O are required to completely melt the original melt + crystal protolith and saturate the melt with fluid. That is, a small amount of volatile fluid can initiate many times its weight in melt produced.

The qualitative model outlined above suggests that olivine may be produced by volatile addition to a melt + solid protolith along a thin zone within the cumulus pile. Because this volatile-enriched zone is not at equilibrium with the surrounding rocks, it is likely that concentration gradients may develop which would result in the transfer of material toward and away from the volatile-enriched region. The selective loss of mafic material from the surrounding rocks could further enhance the production of olivine by moving the bulk composition towards the olivine apex. In this situation, it is possible that the protolith may not melt completely, and olivine will remain on the liquidus.

Finally, because interstitial melt may still be expelled from the cumulate pile by diffusion (if the melting occurs at or near the interface of the magma/cumulate pile) or by convection of the interstitial melt (*e.g.*, Tait *et al.* 1984), then loss of the residual melt produced during fluxing to the overlying magma body can explain the necessary loss of the silica and other components during production of olivine. As with the infiltration metasomatism model of Irvine (1980), once the melt has been equilibrated by reaction with the cumulates at the level of the discontinuity, it may pass through the pile with little additional effect on the overlying cumulates. The effect of mixing of this volatile- and silica-rich melt to the magma within the chamber would depend on the relative amount of material added. Its effect on the composition of the supernatant magma would be expected to be negligible if a small amount of material were added to a large volume of well-mixed magma.

The degree to which the partial melt is retained and not lost to the overlying magma body would govern the extent to which a second generation of pyroxene and plagioclase would develop as interstitial or poikilitic grains. The fact that orthopyroxene encloses not only olivine but other minerals such as sulfide, chromite, and even the Cl-rich apatite (Barnes & Naldrett 1985, Boudreau *et al.* 1986) is consistent with much of the volatile influx occurring above the solidus temperature of the rock.

Cause of PGE-sulfide precipitation

Because sulfur is likely to be an important constituent of the magmatic volatile-fluid phase (*e.g.*, Burnham 1979a,b, Haughton *et al.* 1974), the volatile fluid is also a potential source of sulfide mineralization in the ore zone. In addition, the high Cl concentrations of the fluid greatly enhances its metal transporting capacity (*e.g.*, Holland 1972). Ballhaus & Stumpfl (1986) have reviewed reactions by which a sulfur-bearing fluid may precipitate an immiscible sulfide melt. The reaction they consider to be of fundamental importance involves the dissolution of H_2S from the volatile-fluid phase into the melt (Holloway 1981):

$$H_2S_v + FeO_{melt} + O^{2-}_{melt} = FeS_{melt} + 2\ OH^{-}_{melt} \qquad (2)$$

As noted by Ballhaus & Stumpfl, dissolution of H_2S and the precipitation of immiscible-sulfide melt leads to increased OH^- in the melt, which explains in part the association of sulfides with hydrous minerals. In addition, the reaction may also lead to lower $f(O_2)$ as the reaction proceeds to the right. A simple model for the formation of the ore zone has a volatile fluid exsolving from the footwall and incorporating sulfur and the PGE, the latter being carried as Cl-complexes. Redissolution of this fluid in stratigraphically higher, hot fluid-undersaturated intercumulate melt leads to the precipitation of immiscible PGE-bearing sulfide melt. As suggested below, however, the actual behavior of sulfur is likely to be more complicated.

Variation in mineral modes with reaction progress

A progressive reaction between a cumulate protolith + interstitial melt and an interstitial volatile fluid would be expected to result in regular and predictable variations in the amounts of the mineral phases present in the rocks. Because field and textural evidence implies that the reaction was accompanied by a segregation of plagioclase from mafic phases, modal data from thin section point counts must be interpreted with this in mind. As shown above, addition of vapor to a melt + pyroxene protolith produces olivine by incongruent melting of pyroxene at a fixed magma composition:

$$\underset{\text{opx}}{2MgSiO_3} + \underset{\text{vapor}}{H_2O} \rightarrow \underset{\text{olivine}}{Mg_2SiO_4} + \text{"more melt"} \qquad (3)$$

Using this reaction as a model, it is evident that the molar amount of olivine defines reaction progress, *i.e.*, increasing fluid/rock ratio (*e.g.*, Brimhall 1979).

Molar amounts of mineral phases per kilogram of rock (Table 2) are plotted against the molar olivine abundance in Figure 6. (Not shown is ilmenite, of which approximately 5% is present as a coarse interstitial grain in one section with 54% olivine.) Several caveats must be applied to the strict interpretation of molar olivine abundance with increasing fluid/rock ratio. Melting is not a constant-volume process (although one might expect the volume of the residual solids to monotonically decrease as melting progresses), and the melt phase can be lost to the supernatant magma. In addition, the protolith is not of uniform composition; modal variation is

TABLE 2. MINERAL DATA USED IN CALCULATING FIGURE 6

	molecular wt. (g/mole)	density (g/cm^3)
olivine	155	3.5
plagioclase	275	2.7
low-Ca pyroxene	110	3.3
augite	225	3.2
sulfide	88	4.8
chromite	200	4.5
phlogopite	430	2.9

typical of much of the Banded series. Thus the increase in reaction progress as measured by increasing molar olivine abundance as shown in Figure 6 must be viewed as semiquantitative. Bearing this in mind, however, several generalizations can be drawn which are consistent with textural evidence presented above. The segregation of the mafic and felsic components is indicated by the decreasing modal abundance of plagioclase with increasing modal olivine.

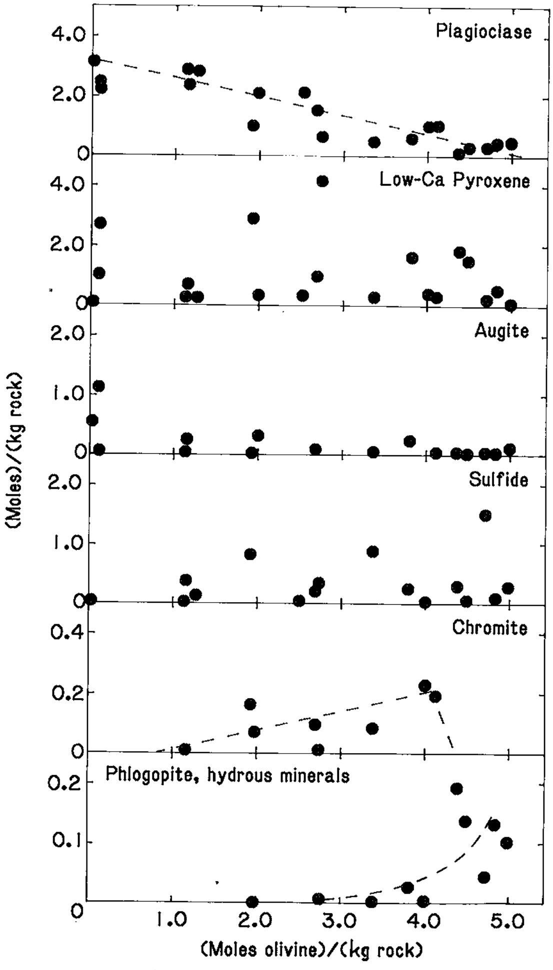

FIG. 6. Variation in the number of moles of mineral phases in 1000 g rock with the variation in the number of moles of olivine. The direction of increase in the fluid/rock ratio is inferred by the production of olivine and with textural evidence discussed in the text. Data were calculated from modal data (obtained by point counting), using the average values for gram molecular weight and density listed in Table 2. Minor amounts of apatite and clinoamphibole, always less abundant than phlogopite, were included with phlogopite in the mode and calculated as phlogopite.

Chromite is restricted to rocks with intermediate amounts of olivine, and is absent in phlogopite-rich rocks. These observations are consistent with the chromite being stable only at intermediate values of fluid/rock ratio, and the outward migration of chromium to form the chromite-rich margins of the pegmatites. The presence of hydrous melt inclusions in chromite is further evidence that the chromite was precipitated from a volatile-enriched melt. The relatively high chromium content of the partial melt could have resulted from the melting of pyroxene. Phlogopite and other hydrous minerals are common only in olivine-rich rock types. Because there are no potassium-bearing phases in the protolith assemblage (except for the insignificant amount in plagioclase), the presence of phlogopite requires the addition of potassium to the system. Sodium must also have been added since interstitial plagioclase in the phlogopite-bearing rocks is unusually albitic (Table 3). This is consistent with experimental evidence and thermochemical calculations (*e.g.*, Hards 1976, Gammon *et al.* 1969, Boudreau *et al.* 1986) that the alkalis are abundant in an exsolving aqueous, Cl-bearing fluid. The modal amounts of pyroxene, especially orthopyroxene, are variable, reflecting late formation of orthopyroxene by crystallization of residual melt and peritectic reactions involving olivine.

To summarize, the paragenetic sequence, from the protolith norites/gabbronorites to the dunites, consists of the following phase assemblages which include interstitial melt (and ignoring the late-formed orthopyroxene and plagioclase in the olivine-bearing rocks):

A) plagioclase + orthopyroxene ± clinopyroxene ± quartz (gabbronorite–norite protolith)
(A′) plagioclase ± orthopyroxene ± clinopyroxene (anorthosite)
B) plagioclase + olivine (troctolite)
C) olivine + chromite + plagioclase (troctolite–dunite)
D) olivine + phlogopite (dunite)

The ideal rock sequence A-D which results from the reaction is shown schematically in the μ-μ-μ diagram in Figure 7. This diagram qualitatively displays much the same information as a liquidus phase diagram, and it illustrates that the rock sequence need not be the result of crystallization on a multiply-saturated liquidus surface but may instead be generated by subliquidus reaction. The phlogopite "wedge" shown in the bottom of the Figure will intrude farther into the phase space with increasing activity of potassium and H_2O, and will further separate plagioclase from the olivine phase volumes. Note also that a result of mafic "leaching" is that the heavy line A–B lies entirely within the plagioclase phase volume, and separates all (gabbro)noritic assemblages from the olivine-bearing (troctolitic) assemblages.

Variation in sulfur and oxygen fugacity with reaction progress

The mineral assemblages of OBZ I allow a semi-quantitative interpretation of the variation of the oxygen and sulfur fugacity accompanying the formation of the secondary olivine. Based on the mineral parageneses noted above, $f(S_2)$ and $f(O_2)$ are controlled by the following reactions:

$$\tfrac{1}{2}O_2 + \underset{\text{po}}{FeS} + \underset{\text{opx}}{FeSiO_3} = \underset{\text{olivine}}{Fe_2SiO_4} + \tfrac{1}{2}S_2 \tag{4}$$

$$\tfrac{1}{2}O_2 + \underset{\text{olivine}}{3Fe_2SiO_4} = \underset{\text{spinel}}{Fe_3O_4} + \underset{\text{opx}}{3FeSiO_3} \tag{5}$$

$$2O_2 + \underset{\text{po}}{3FeS} = \underset{\text{spinel}}{Fe_3O_4} + \tfrac{3}{2}S_2 \tag{6}$$

$$\underset{\text{plag}}{KAlSi_3O_8} + \underset{\text{spinel}}{Fe_3O_4} + H_2O = \underset{\text{phlogopite}}{KFe_3AlSi_3O_{10}(OH)_2} + \tfrac{1}{2}O_2 \tag{7}$$

$$\underset{\text{plag}}{KAlSi_3O_8} + \underset{\text{po}}{3FeS} + H_2O + \tfrac{1}{2}O_2 = \underset{\text{phlogopite}}{KFe_3AlSi_3O_{10}(OH)_2} + \tfrac{3}{2}S_2 \tag{8}$$

Precise interpretation of the changes in $f(S_2)$ and $f(O_2)$ are not possible because $f(H_2O)$, temperature, and pyrrhotite composition are not well constrained. In addition, extensive unmixing and re-equilibration that the high-temperature mineral phases have undergone during cooling limit direct application of the calculations.

The sulfur- and oxygen-controlling reactions 4–8 above as well as the reaction sequence assemblages A–D are shown on the log $f(S_2)$ *versus* log $f(O_2)$ diagram in Figure 8 (uncertainty in the temperature and the activity relationships will not affect the basic chemographic relationships). Shown schematically by the heavy line is the inferred change in the $f(S_2)$ and $f(O_2)$ with increasing extent of reaction (line A–D). It is seen that, as the reaction proceeds, the reaction is accompanied by a reduction in both $f(S_2)$ and $f(O_2)$. The decrease in $f(S_2)$ with reaction progress is consistent with the interpretation that sulfide was precipitated early in the course of the reaction (as seen in the presence of mineralized norites and gabbronorites in the J-M Reef, *e.g.* Bow *et al.* 1982), and was remobilized at higher fluid–rock

TABLE 3. CHEMICAL COMPOSITION OF CUMULUS AND INTERSTITIAL PLAGIOCLASE FROM THE MINNEAPOLIS ADIT

		cumulus MA189	interstitial, 5104WL	with phlogopite 5104EX
SiO_2	wt. %	47.19	48.60	55.95
Al_2O_3		33.61	32.45	27.66
FeO		0.47	0.29	0.20
MgO		0.02	na	0.00
CaO		17.05	15.87	9.71
Na_2O		1.85	2.70	6.23
K_2O		0.09	na	0.10
Total		100.27	99.91	99.84
Cations per 8 oxygen atoms:				
Si		2.165	2.229	2.522
Al		1.818	1.754	1.470
Fe		0.018	0.011	0.008
Mg		0.001	-	0.000
Ca		0.838	0.780	0.469
Na		0.164	0.240	0.545
K		0.005	-	0.006

Notes: na means "not analyzed". Conditions of analysis: 15 kV, 25 nA sample current, 10-μm beam diameter, 20-s counting time, average of 3 points per grain.

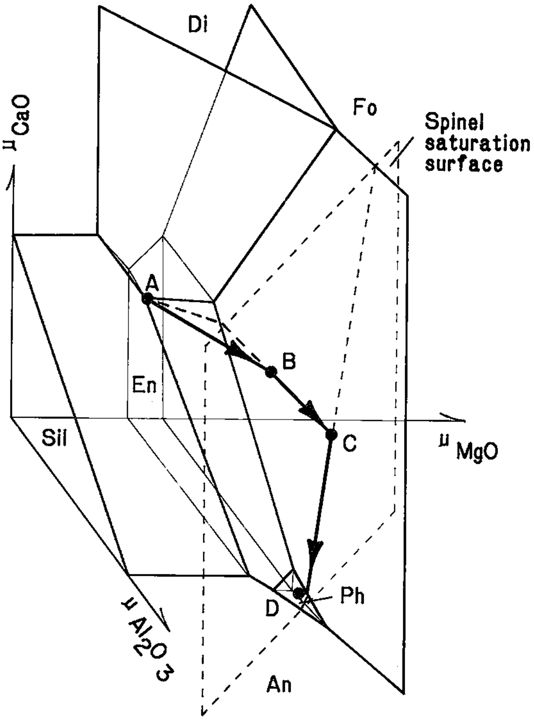

FIG. 7. Qualitative diagram of the relative stabilities of mineral phases in the system CaO–MgO–Al_2O_3–SiO_2–K_2O–H_2O, with variation in the chemical potential of the component oxides CaO, MgO and Al_2O_3, all other components assumed fixed. All reactions shown balanced on silica, with spinel shown as a dashed saturation plane. Abbreviations: Sil silica, En enstatite, Fo forsterite, An anorthite, Ph phlogopite. The points A–B–C–D denote the paragenetic sequence listed in the text, and the heavy lines illustrate one possible chemical-potential path to produce the observed sequences of rocks. Note that heavy solid-line segment A–B lies entirely within the plagioclase phase volume: the dashed line segment A–B illustrates yet one other path that lies entirely on multiple-saturation boundaries.

ratios to give the discontinuous distribution of ore within the pegmatitic, olivine-rich portions of the Minneapolis adit (Bow *et al.* 1982). The remobilization of sulfide outward from the volatile-enriched regions is also consistent with the distribution of the ore in the West Fork adit, where sulfides are preferentially located in the anorthositic and troctolitic rocks directly above the pegmatitic olivine-rich layer (Mann & Lin 1985).

On cooling, the olivine-free assemblages will eventually intercept the pyrite solvus and exsolve pyrite as part of the exsolution assemblage, whereas the olivine (± phlogopite)-rich assemblages will not (Fig. 9). Using reaction (4), oxygen-fugacity contours can be drawn on this Figure (dashed lines) for the spinel + sulfide-bearing assemblages, and are used to show the range of intrinsic oxygen-fugacity data of Elliott *et al.* (1982). Bow *et al.* (1982) and Barnes & Naldrett (1985) noted that the sulfide assemblage now observed in the rocks was formed by unmixing from a high-temperature monosulfide solution, and that pyrite with an exsolution texture is common only in mineralized norites and gabbronorites of the ore zone. Because the pyrite field will begin to appear between the pyrrhotite and condensed-sulfur fields at temperatures below 742°C, the pyrite-bearing assemblages are consistent with a higher initial sulfur fugacity in the olivine-absent assemblages than in the olivine-bearing assemblages without exsolved pyrite.

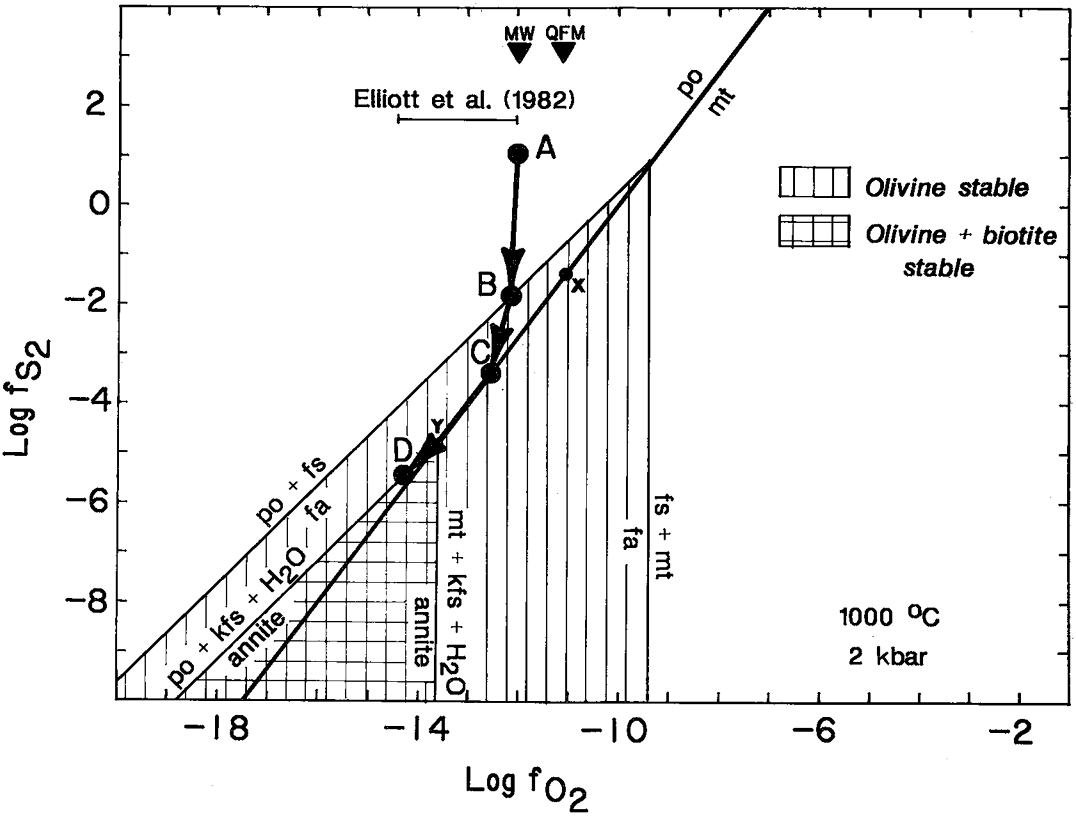

FIG. 8. Stability of phase assemblages as a function of $f(S_2)$ and $f(O_2)$ at 1000°C and 2 kbar. Compiled using the thermochemical data of Helgeson *et al.* (1978). Abbreviations: po pyrrhotite, mt magnetite, kfs potassium feldspar, fa fayalite, fs ferrosilite. The regions of olivine stability and olivine + phlogopite stability are shown by the ruled and crossruled regions, respectively. The fa–fs and po–mt boundaries have incorporated the following assumptions: $a(\text{fs})^{\text{opx}} = 0.27$; $a(\text{fa})^{\text{ol}} = 0.09$; $a(\text{po}) = 1.0$; $a(\text{mt})^{\text{chrome spinel}} = 0.15$. The relative position of the annite field is temperature-dependent, and the boundaries are shown for pure end-member phases. The points A–D denote the paragenetic sequence listed in the text. The range of intrinsic oxygen fugacity for cumulus plagioclase from the Lower Banded series, as measured by Elliott *et al.* (1982), is also shown. The magnetite–wustite (MW) and quartz–fayalite–magnetite (QFM) buffers are shown for reference. The points X and Y are shown varying through temperature in Figure 9.

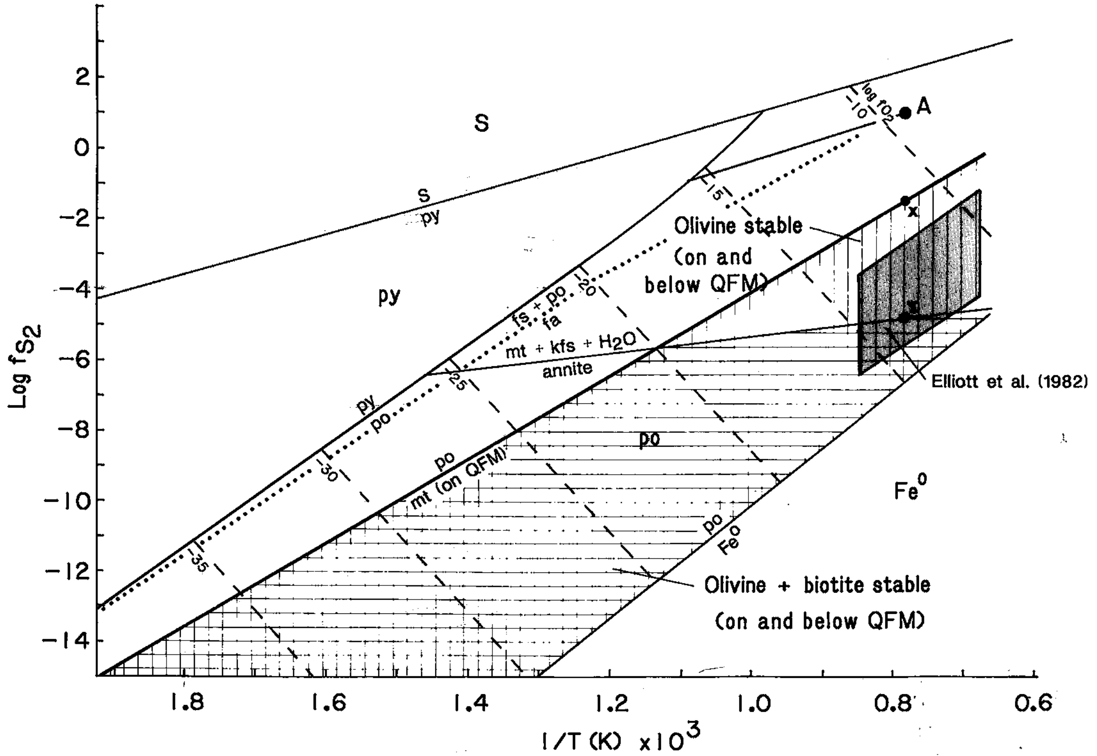

FIG. 9. Mineral stabilities as a function of log $f(S_2)$ and 1/T(K). Abbreviations as in the previous figure, with Fe° iron, py pyrite, S condensed sulfur. The stability of the silicate–oxide–sulfide assemblages from Figure 8 are plotted with the phase relations from the system Fe–S (from Scott 1974), in part schematic. The mt–po reaction is used to contour $f(O_2)$ (dashed lines) for those assemblages which contain both of these phases. Point X of this and Figure 8, which is the po–mt boundary on QFM at 1000°C, is shown varying with temperature as the heavy solid line. Similarly, point Y of this and Figure 8, which is the maximum stability limit of annite at 1000°C, is also shown varying with temperature. The maximum stability of olivine in the presence of po + mt is shown as the dotted line. The sulfide-bearing olivine + chrome spinel and olivine + phlogopite + chrome spinel assemblages have the sulfur and oxygen fugacities both controlled by the presence of sulfide, silicate, or oxide phases, and do not intersect the pyrite solvus on cooling, particularly for oxygen fugacities on or below QFM. In contrast, the sulfur fugacity of assemblage A (olivine and oxides absent) is controlled only by the presence of pyrrhotite, and hence follows a pyrrhotite isopleth to intersect the pyrite solvus on cooling (solid line). The equivalent range of intrinsic oxygen fugacities measured in cumulus plagioclase from the Lower Banded series (Elliott *et al.* 1982) is shown by the shaded field for spinel–sulfide-bearing assemblages.

CONCLUSIONS

A summary model

A schematic model for the formation of the lithologic sequences of the J-M Reef is as follows: at some point in the solidification of the cumulus pile, a lithologic discontinuity within the cumulus sequence acted as a trap to the upward migration of volatile-rich fluids. The discontinuity could have resulted from the injection of a compositionally distinct (vapor-undersaturated) magma. With increasing infiltration of volatile fluid from lower cumulates, an increasing amount of partial melting, reaction of the cumulus crystals, and material transport between the volatile-enriched region and the surrounding cumulates was to be expected. Cumulus plagioclase dissolved incongruently to produce reverse-zoned and rounded grains, and the destruction of pyroxene produced olivine, chromite, and local ilmenite. Transfer of mafic components toward the fluid-rich areas and the plagioclase components outward resulted in the characteristic olivine-rich rock/anorthosite association. The thickness of the reaction zone increased with increasing addition of fluid. The latent heat of fusion required for partial melting induced by volatile fluxing could have been supplied by the surrounding rocks and the supernatant magma. Hence, the surrounding rocks must have undergone increased crystallization while the volatile-enriched zone became increasingly molten. This would have further enhanced permeability differences, and restricted the volatile-enriched region to a narrow layer. In extreme instances, the increasingly molten rocks may have been deformed or formed apophyses into the rigid marginal rocks. Loss of silica from the crystal pile was achieved by convective or diffusive expulsion of the interstitial melt. On eventual cooling, crystallization of any residual partial melt generated during melting, and not lost to the overlying magma body, led to the second generation of coarse orthopyroxene and plagioclase which enclosed all earlier-formed phases. The final result is a regionally stratabound zone of pegmatitic rocks with sulfide (and chromite) preferentially located in the marginal regions of low to moderate fluid/rock ratio. It is suggested that the characteristic thin (1–2 cm) layers of sulfides and chromite which occur at the margins of the Merensky pegmatoid (*cf.* Naldrett 1981) could have formed in an analogous manner.

Comparison with other models

In many respects, the model presented here has similarities with previous models. Although the infiltration metasomatic model of Irvine (1980) deals primarily with the infiltration of melt during compaction of the cumulate pile, the effect of an infiltrating fluid driven by fluid buoyancy is an analogous process. In the Merensky Reef, the presence of high-temperature fluid inclusions and graphitic pegmatites is evidence that a volatile fluid in addition to melt was present (*e.g.*, Ballhaus & Stumpfl 1985a, 1986). In the Stillwater Complex the evidence for the presence of a separate volatile fluid instead of a volatile-enriched residual liquid is indirect, and includes the presence of pegmatites which may be unusually sulfur-rich. Boudreau *et al.* (1986) argued that unusually high $Cl/(Cl+F+OH)$ ratios observed in the J-M Reef and Bushveld Critical Zone hydrous phases cannot simply have been due to the crystallization of trapped melt; the high ratios must have involved the preferential addition of Cl to the zones, which is most readily accomplished by redissolution of a volatile-fluid phase as described here. The model proposed by Boudreau *et al.* (1986) for the enrichment in Cl in these zones is similar to the concept of constitutional zone-refining in layered intrusions as recently was proposed by McBirney (1987). The alternative model, in which a volatile-enriched melt is displaced upward and reacts with anhydrous silicates, cannot in itself cause changes in the Cl/F ratio of the melt. In addition, Cl-rich fluids are a recognized metal-transporting medium, whereas the transport properties of a volatile-enriched interstitial melt remain to be demonstrated.

Dunn (1986), in a study of the oxygen isotopic systematics of the Stillwater Complex, has shown that the Stillwater rocks retain a mantle signature, and hence have not experienced a large-scale circulation of meteoric water as has apparently occurred in the Skaergaard Intrusion (Taylor & Forrester 1979). Dunn has also suggested that the ^{18}O depletions associated with the olivine-bearing zones of the Banded series are consistent with a magmatically derived, late-stage fluid in these zones.

In a related model, Elliott *et al.* (1982) and Buntin *et al.* (1985) have suggested that volatile fluids may actually be injected and mixed into the magma chamber directly. One would expect that this addition of volatiles to the magma in the chamber would depress the liquidus and solidus relations in a manner analogous to the mechanism proposed here, and hence partial melting of the floor rocks should be an expected consequence of these models as well.

ACKNOWLEDGEMENTS

This work was supported by NASA grant NAG 9-84 (I.S. McCallum, P.I.). Critical reviews of this manuscript by I.S. McCallum, Norman Page and an anonymous reviewer resulted in considerable improvement and are very much appreciated.

REFERENCES

ADAMS, J.B. (1968): Differential solution of plagioclase in supercritical water. *Amer. Mineral.* **53**, 1603-1613.

BALLHAUS, C.G. & STUMPFL, E.F. (1985a): Occurrence and petrological significance of graphite in the Upper Critical Zone, western Bushveld Complex, South Africa. *Earth Planet. Sci. Lett.* **74**, 58-68.

_____ & _____ (1985b): Fluid inclusions in Merensky and Bastard Reefs, western Bushveld Complex. *Can. Mineral.* **23**, 294 (abstr.).

_____ & _____ (1985c): Graphite, platinum and the C–O–H–S system. *Can. Mineral.* **23**, 293 (abstr.).

_____ & _____ (1986): Sulfide and platinum mineralization in the Merensky Reef: evidence from hydrous silicates and fluid inclusions. *Contr. Mineral. Petrology* **94**, 193-204.

BARNES, S.J. (1983): *Petrology and Geochemistry of a Portion of the Howland (J.-M.) Reef of the Stillwater Complex, Montana.* Unpubl. Ph.D. Dissertation, Univ. Toronto, Toronto, Ont.

_____ & NALDRETT, A.J. (1985): Geochemistry of the J-M (Howland) Reef of the Stillwater Complex, Minneapolis adit area. I. Sulfide chemistry and sulfide-olivine equilibrium. *Econ. Geol.* **80**, 627-645.

_____ & _____ (1986): Geochemistry of the J-M Reef of the Stillwater Complex, Minneapolis Adit area.

II. Silicate mineral chemistry and petrogenesis. *J. Petrology* **27**, 791-826.

Boudreau, A.E., Mathez, E.A. & McCallum, I.S. (1986): The halogen geochemistry of the Stillwater and Bushveld Complexes: evidence for the transport of the platinum-group elements by Cl-rich fluids. *J. Petrology* **27**, 967-986.

Bow, C., Wolfgram, D., Turner, A., Barnes, S., Evans, J., Zdepski, M. & Boudreau, A. (1982): Investigations of the Howland Reef of the Stillwater Complex, Minneapolis adit area; stratigraphy, structure, and mineralization. *Econ. Geol.* **77**, 1481-1492.

Bowen, N.L. & Tuttle, O.F. (1949): The system MgO - SiO_2 - H_2O. *Geol. Soc. Amer. Bull.* **60**, 439-460.

Brimhall, G.H. (1979): Lithologic determination of mass transfer mechanism of multiple stage porphyry copper mineralization at Butte, Montana: vein formation by hypogene leaching and enrichment of potassium-silicate protore. *Econ. Geol.* **74**, 556-589.

Buntin, T.J., Grandstaff, D.E., Ulmer, G.C. & Gold, D.P. (1985): A pilot study of geochemical and redox relationships between potholes and adjacent normal Merensky Reef of the Bushveld Complex. *Econ. Geol.* **80**, 975-988.

Burnham, C.W. (1979a): Magmas and hydrothermal fluids. *In* Geochemistry of Hydrothermal Ore Deposits (H.L. Barnes, ed.). John Wiley & Sons, New York.

______ (1979b): The importance of volatile constituents. *In* The Evolution of the Igneous Rocks (H.S. Yoder, ed.). Fiftieth Anniversary Perspectives, Princeton University Press, Princeton, N.J.

Cameron, E.N. & Desborough, G.A. (1964): Origin of certain magnetite-bearing pegmatites in the eastern part of the Bushveld Complex, South Africa. *Econ. Geol.* **59**, 197-225.

Campbell, I.H., Naldrett, A.J. & Barnes, S.J. (1983): A model for the origin of the platinum-rich sulfide horizons in the Bushveld and Stillwater complexes. *J. Petrology* **24**, 133-165.

Conn, H.K. (1979): The Johns-Manville platinum-palladium prospect, Stillwater Complex, Montana, U.S.A. *Can. Mineral.* **17**, 463-469.

Dunn, T. (1986): An investigation of the oxygen isotope geochemistry of the Stillwater Complex. *J. Petrology* **27**, 987-998.

Elliott, W.C., Grandstaff, D.E., Ulmer, G.C., Buntin, T. & Gold, D.P. (1982): An intrinsic oxygen fugacity study of the platinum-carbon associations in layered intrusions. *Econ. Geol.* **77**, 1493-1510.

Gammon, J.B., Borcsik, M. & Holland, H.D. (1969): Potassium-sodium ratio in aqueous solutions and coexisting silicate melts. *Science* **163**, 179-181.

Hards, N. (1976): Distribution of elements between the fluid phase and silicate melt phase of granites and nepheline syenites. *In* Progress in Experimental Petrology (G.M. Biggar, ed.). Natural Environment Research Council Publication series D 6.

Haughton, D.R., Roeder, P.L. & Skinner, B.J. (1974): Solubility of sulfur in mafic magmas. *Econ. Geol.* **69**, 451-462.

Helgeson, H.C., Delany, J.M., Nesbitt, H.W. & Bird, D.K. (1978): Summary and critique of the thermodynamic properties of rock-forming minerals. *Amer. J. Sci.* **278A**.

Holland, H.D. (1972): Granites, solutions and base metal deposits. *Econ. Geol.* **67**, 281-301.

Holloway, J.R. (1981): Volatile interactions in magmas. *In* Thermodynamics of minerals and melts: Advances in physical geochemistry 1 (R.C. Newton, A. Navrotsky & B.J. Wood, eds.). Springer-Verlag, New York.

Irvine, T.N. (1980): Magmatic infiltration metasomatism, double-diffusive fractional crystallization, and adcumulus growth in the Muskox intrusion and other layered intrusions. *In* Physics of Magmatic Processes (R.B. Hargraves, ed.). Princeton University Press, Princeton, New Jersey, 325-383.

______, Keith, D.W. & Todd, S.G. (1983): The J-M platinum-palladium reef of the Stillwater Complex, Montana: II. Origin by double-diffusive convective magma mixing and implications for the Bushveld Complex. *Econ. Geol.* **78**, 1287-1334.

Johan, Z. & Watkinson, D.H. (1985): Significance of a fluid phase in platinum-group-element concentration: evidence from the Critical Zone, Bushveld Complex. *Can. Mineral.* **23**, 305-306 (abstr.).

Kushiro, I. (1975): On the nature of silicate melt and its significance in magma genesis: regularities in the shift of the liquidus boundaries involving olivine, pyroxene, and silica minerals. *Amer. J. Sci.* **275**, 411-431.

______, Yoder, H.S. & Nishikawa, M. (1968): Effect of water on the melting of enstatite. *Geol. Soc. Amer. Bull.* **79**, 1685-1692.

Leroy, L.W. (1985): Troctolite-anorthosite zone I and the J-M Reef: Frog pond adit to the Graham Creek area. *In* The Stillwater Complex, Montana: Geology and Guide (G.K. Czamanske & M.L. Zientek, eds.). *Montana Bur. Mines Geol. Spec. Publ.* **92**, 325-333.

Longhi, J., Walker, D. & Hays, J.F., (1976): Fe and Mg in plagioclase. *Proc. Lunar Sci. Conf. 7th*, 1281-1300.

MANN, E.L. & LIN, C.-P. (1985): Geology of the West Fork adit. *In* The Stillwater Complex, Montana: Geology and Guide (G.K. Czamanske & M.L. Zientek, eds.). *Montana Bur. Mines Geol. Spec. Publ.* **92**, 247-252.

______, LIPIN, B.R., PAGE, N.J, FOOSE, M.P. & LOFERSKI, P.J. (1985): Guide to the Stillwater Complex exposed in the West Fork area. *In* The Stillwater Complex, Montana: Geology and Guide (G.K. Czamanske & M.L. Zientek, eds.). *Montana Bur. Mines Geol. Spec. Publ.* **92**, 231-246.

MCBIRNEY, A.R. (1987): Constitutional zone refining of layered intrusions. *In* Origins of Igneous Layering (I. Parsons, ed.). D. Reidel, Dordrecht, Holland, 437-452.

MCCALLUM, I.S. (1968): *Equilibrium Relationships Among the Coexisting Minerals in the Stillwater Complex, Montana.* Unpubl. Ph.D. thesis, Univ. Chicago, Chicago, Ill.

______, RAEDEKE, L.D. & MATHEZ, E.A. (1980): Investigations of the Stillwater Complex. Part I. Stratigraphy and structure of the Banded zone. *Amer. J. Sci.* **280A**, 59-87.

NALDRETT, A. (1981): Platinum-group element deposits. *In* Platinum-Group Elements: Mineralogy, Geology, Recovery (L.J. Cabri, ed.). *Can. Inst. Mining Metall. Spec. Vol.* **23**, 197-232.

ORVILLE, P.M. (1972): Plagioclase cation exchange equilibria with aqueous chloride solution: results at 700°C and 2000 bars in the presence of quartz. *Amer. J. Sci.* **272**, 234-272.

RAEDEKE, L.D. & MCCALLUM, I.S. (1984): Investigations in the Stillwater Complex: Part II. Petrology and petrogenesis of the Ultramafic series. *J. Petrology* **25**, 395-420.

SCHIFFRIES, C.M. (1982): The petrogenesis of a platiniferous dunite pipe in the Bushveld Complex: infiltration metasomatism by a chloride solution. *Econ. Geol.* **77**, 1439-1453.

______ (1984): The Bushveld hydrothermal system. *27th Int. Geol. Cong. Abstr.* **2**, 385-386.

SCOTT, S.D. (1974): The Fe-S system. *In* Sulfide Mineralogy (P.H. Ribbe, ed.). *Mineral. Soc. Amer. Rev. Mineral.* **1**, CS21-CS40.

SMITH, J.V. (1983): Some chemical properties of feldspars. *In* Feldspar Mineralogy (P.H. Ribbe, ed.). *Mineral. Soc. Amer. Rev. Mineral.* **2**, 281-296.

STUMPFL, E.F. & RUCKLIDGE, J.C. (1982): The platiniferous dunite pipes of the eastern Bushveld. *Econ. Geol.* **77**, 1419-1431.

TAIT, S.R., HUPPERT, H.E. & SPARKS, R.S.J. (1984): The role of compositional convection in the formation of adcumulate rocks. *Lithos* **17**, 139-146.

TAYLOR, H.P. & FORRESTER, R.W. (1979): An oxygen and hydrogen isotope study of the Skaergaard intrusion and its country rocks: a description of a 55-m.y. old fossil hydrothermal system. *J. Petrology* **20**, 355-419.

TODD, S.G., KEITH, D.W., LEROY, L.W., SCHISSEL, D.J., MANN, E. L. & IRVINE, T.N. (1982): The J-M platinum-palladium reef of the Stillwater Complex, Montana: I. Stratigraphy and petrology. *Econ. Geol.* **77**, 1454-1480.

TURNER, A., WOLFGRAM, D. & BARNES, S.J. (1985): Geology of the Stillwater County sector of the J-M Reef, including the Minneapolis adit. *In* The Stillwater Complex Montana: Geology and Guide (G.K. Czamanske & M.L. Zientek, eds.). *Montana Bur. Mines Geol. Spec. Publ.* **92**, 210-230.

Received November 26, 1986; revised manuscript accepted May 29, 1987.